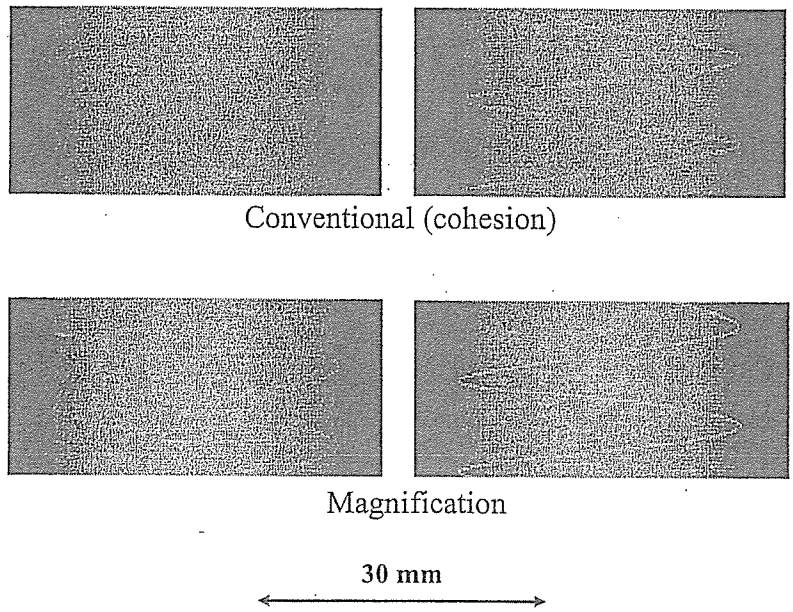

Figure 8. Radiograms of tungsten wires coiled around PMMA rods.

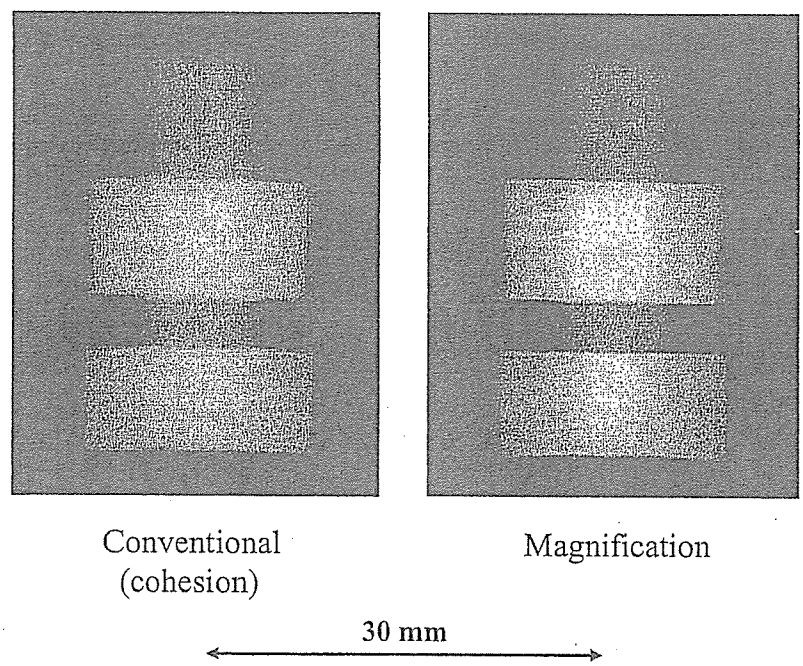

Figure 9. Radiograms of a set of a plastic bolt and a nut.

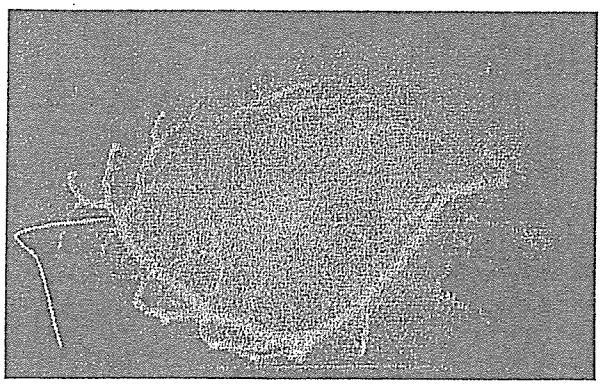

Figure 10: Angiogram of an extracted rabbit heart using iodine microspheres.

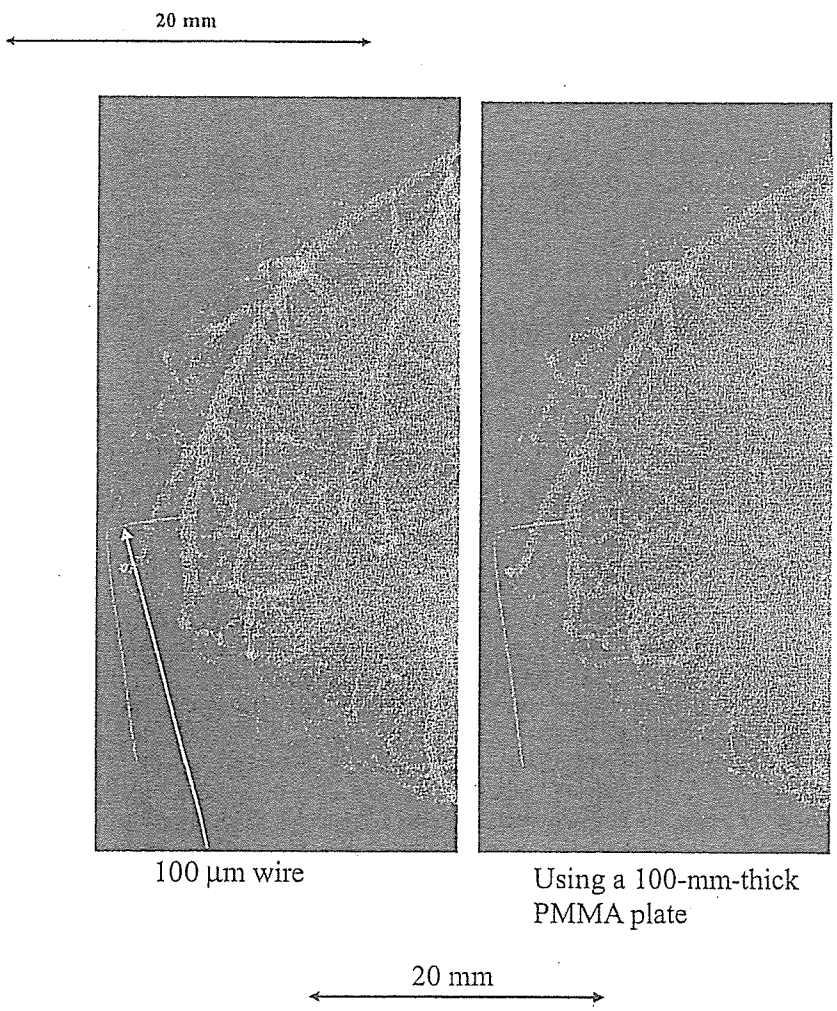

Figure 11. Angiograms of an extracted dog heart.

5. CONCLUSIONS AND OUTLOOK

In summary, we employed an x-ray generator with a 100-μm-focus tungsten tube and performed enhanced magnification angiography including phase-contrast effect using narrow-photon-energy bremsstrahlung x-rays with a peak photon energy of approximately 38 keV, which can be absorbed easily by iodine-based contrast media. The bremsstrahlung x-ray intensity substantially increased with increases in the tube voltage, and the tube voltage was determined as 60 kV in order to increase the image contrast. In enhanced angiography, although we obtained almost absorption-contrast images, phase-contrast effect may be added in cases where low-density media are employed.

Because the sampling pitch of the CR system is 87.5 μm, we obtained spatial resolutions of approximately 50 μm using 3-time magnification imaging even when a 100-μm-focus tube was employed. In order to observe fine blood vessels of less than 100 μm, the spatial resolution of the CR system should be improved to 43.8 μm (Konica Minolta Regius 190), and the iodine density should be increased.

At a tube voltage of 60 kV and a current of 0.50 mA, the maximum number of photons was approximately 4×10^7 photons/cm^2·s at 1.0 m from the source, and the photon count rate can be increased easily using a rotating anode microfocus tube developed by Hitachi Medical Corporation. Recently, the maximum electric power of the microfocus x-ray tube has been increasing, and the kilowatt-range tube can be realized. Therefore, the dynamic magnification radiography is possible using a flat panel detector with a pixel size of less than 100 μm.

ACKNOWLEDGMENTS

This work was supported by Grants-in-Aid for Scientific Research (13470154, 13877114, 16591181, and 16591222) and Advanced Medical Scientific Research from MECSST, Health and Labor Sciences Research Grants (RAMT-nano-001, RHGTEFB-genome-005 and RHGTEFB-saisei-003), Grants from the Keiryo Research Foundation, The Promotion and Mutual-Aid Corporation for Private Schools of Japan, Japan Science and Technology Agency (JST), and the New Energy and Industrial Technology Development Organization (NEDO, Industrial Technology Research Grant Program in '03).

REFERENCES

1. R. Germer, "X-ray flash techniques," *J. Phys. E: Sci. Instrum.*, **12**, 336-350, 1979.
2. E. Sato, Y. Hayasi, R. Germer, E. Tanaka, H. Mori, T. Kawai, T. Ichimaru, S. Sato, K. Takayama and H. Ido, "Portable x-ray generator utilizing a cerium-target radiation tube for angiography," *J. Electron Spectrosc. .Related Phenom.*, **137-140**, 699-704, 2004.
3. E. Sato, E. Tanaka, H. Mori, T. Kawai, T. Ichimaru, S. Sato, K. Takayama and H. Ido, "Demonstration of enhanced K-edge angiography using a cerium target x-ray generator," *Med. Phys*, **31**, 3017-3021, 2004.
4. E. Sato, S. Kimura, S. Kawasaki, H. Isobe, K. Takahashi, Y. Tamakawa and T. Yanagisawa, "Repetitive flash x-ray generator utilizing a simple diode with a new type of energy-selective function," *Rev. Sci. Instrum.*, **61**, 2343-2348, 1990.
5. A. Shikoda, E. Sato, M. Sagae, T. Oizumi, Y. Tamakawa and T. Yanagisawa, "Repetitive flash x-ray generator having a high-durability diode driven by a two-cable-type line pulser," *Rev. Sci. Instrum.*, **65**, 850-856, 1994.
6. E. Sato, K. Takahashi, M. Sagae, S. Kimura, T. Oizumi, Y. Hayasi, Y. Tamakawa and T. Yanagisawa, "Sub-kilohertz flash x-ray generator utilizing a glass-enclosed cold-cathode triode," *Med. & Biol. Eng. & Comput.*, **32**, 289-294, 1994.
7. K. Takahashi, E. Sato, M. Sagae, T. Oizumi, Y. Tamakawa and T. Yanagisawa, "Fundamental study on a long-duration flash x-ray generator with a surface-discharge triode," *Jpn. J. Appl. Phys.*, **33**, 4146-4151, 1994.
8. E. Sato, Y. Hayasi, R. Germer, E. Tanaka, H. Mori, T. Kawai, T. Ichimaru, K. Takayama and H. Ido, "Quasi-monochromatic flash x-ray generator utilizing weakly ionized linear copper plasma," *Rev. Sci. Instrum.*, **74**, 5236-5240, 2003.
9. E. Sato, Y. Hayasi, R. Germer, E. Tanaka, H. Mori, T. Kawai, T. Ichimaru, S. Sato, K. Takayama and H. Ido, "Sharp characteristic x-ray irradiation from weakly ionized linear plasma," *J. Electron Spectrosc. Related Phenom.*, **137-140**, 713-720, 2004.
10. E. Sato, E. Tanaka, H. Mori, T. Kawai,S. Sato and K. Takayama, "Clean monochromatic x-ray irradiation from weakly ionized linear copper plasma," *Opt. Eng.*, **44**, 049002-1-6, 2005.
11. E. Sato, M. Sagae, E. Tanaka, Y. Hayasi, R. Germer, H. Mori, T. Kawai, T. Ichimaru, S. Sato, K. Takayama and H. Ido: Quasi-monochromatic flash x-ray generator utilizing a disk-cathode molybdenum tube, *Jpn. J. Appl. Phys.*, **43**, 7324-7328, 2004.

12. E. Sato, E. Tanaka, H. Mori, T. Kawai, T. Ichimaru, S. Sato, K. Takayama and H. Ido, "Compact monochromatic flash x-ray generator utilizing a disk-cathode molybdenum tube," *Med. Phys.*, **32**, 49-54, 2005.
13. A. Momose, T. Takeda, Y. Itai and K. Hirano, "Phase-contrast x-ray computed tomography for observing biological soft tissues," *Nature Medicine*, **2**, 473-475, 1996.
14. M. Ando, A. Maksimenko, H. Sugiyama, W. Pattanasiriwisawa, K. Hyodo and C. Uyama, "A simple x-ray dark- and bright- field imaging using achromatic Laue optics, *Jpn. J. Appl. Phys.*, **41**, L1016-L1018, 2002.
15. H. Mori, K. Hyodo, E. Tanaka, M. U. Mohammed, A. Yamakawa, Y. Shinozaki, H. Nakazawa, Y. Tanaka, T. Sekka, Y. Iwata, S. Honda, K. Umetani, H. Ueki, T. Yokoyama, K. Tanioka, M. Kubota, H. Hosaka, N. Ishizawa and M. Ando, "Small-vessel radiography in situ with monochromatic synchrotoron radiation," *Radiology*, **201**, 173-177, 1996.
16. K. Hyodo, M. Ando, Y. Oku, S. Yamamoto, T. Takeda, Y. Itai, S. Ohtsuka, Y. Sugishita and J. Tada, "Development of a two-dimensional imaging system for clinical applications of intravenous coronary angiography using intense synchrotron radiation produced by a multipole wiggler," *J. Synchrotron Rad.*, **5**, 1123-1126, 1998.
17. E. Sato, K. Sato, T. Usuki and Y. Tamakawa, "Film-less computed radiography system for high-speed imaging," *Ann. Rep. Iwate Med. Univ. Sch. Lib. Arts and Sci.*, **35**, 13-23, 2000.
18. A. Ishisaka, H. Ohara and C. Honda, "A new method of analyzing edge effect in phase contrast imaging with incoherent x-rays," *Opt. Rev.*, **7**, 566-572, 2000.
19. E. Sato, Y. Hayasi, R. Germer, E. Tanaka, H. Mori, T. Kawai, T. Ichimaru, S. Sato, K. Takayama and H. Ido, "Portable x-ray generator utilizing a cerium-target radiation tube for angiography," *J. Electron Spectrosc. Related Phenom.*, **137-140**, 699-704, 2004.
20. E. Sato, E. Tanaka, H. Mori, T. Kawai, T. Ichimaru, S. Sato, K. Takayama and H. Ido, "Demonstration of enhanced K-edge angiography using a cerium target x-ray generator," *Med. Phys*, **31**, 3017-3021, 2004.
*dresato@iwate-med.ac.jp; phone +81-19-651-5111; fax +81-19-654-9282

原子核研究
Vol. 49 No. 5
研究会報告

Conventional enhanced K-edge angiography utilizing cerium x-ray generator

Eiichi Sato[a], Akira Yamadera[b], Toshio Ichimaru[b], Etsuro Tanaka[c], Hidezo Mori[d], Toshiaki Kawai[e], Takashi Inoue[f], Akira Ogawa[f], Shigehiro Sato[g], Kazuyoshi Takayama[h] and Hideaki Ido[i]

[a] Department of Physics, Iwate Medical University, 3-16-1 Honchodori, Morioka 020-0015, Japan

[b] Department of Radiological Technology, School of Health Sciences, Hirosaki University, 66-1 Honcho, Hirosaki 036-8564, Japan

[c] Department of Nutritional Science, Faculty of Applied Bio-science, Tokyo University of Agriculture, 1-1-1 Sakuragaoka, Setagaya-ku 156-8502, Japan

[d] Department of Cardiac Physiology, National Cardiovascular Center Research Institute, 5-7-1 Fujishirodai, Suita, Osaka 565-8565, Japan

[e] Electron Tube Division #2, Hamamatsu Photonics K. K., 314-5 Shimokanzo, Toyooka Village, Iwata-gun 438-0193, Japan

[f] Department of Neurosurgery, School of Medicine, Iwate Medical University, 19-1 Uchimaru, Morioka 020-8505, Japan

[g] Department of Microbiology, School of Medicine, Iwate Medical University, 19-1 Uchimaru, Morioka 020-8505, Japan

[h] Shock Wave Research Center, Institute of Fluid Science, Tohoku University, 2-1-1 Katahira, Sendai 980-8577, Japan

[i] Department of Applied Physics and Informatics, Faculty of Engineering, Tohoku Gakuin University, 1-13-1 Chuo, Tagajo 985-8537, Japan

Abstract

The cerium-target x-ray tube is useful in order to perform cone-beam K-edge angiography because Kα rays from the cerium target are absorbed effectively by iodine-based contrast media. The maximum tube voltage and current were 65 kV and 0.40 mA, respectively, and the focal-spot sizes were approximately 1×1 mm. Sharp cerium Kα lines were left using a barium sulfate filter, and the x-ray

intensity was 16.8 μGy/s at 1.0 m from the source with a tube voltage of 60 kV and a current of 0.40 mA. Angiography was performed using iodine-based microspheres 15 μm in diameter. In angiography of non-living animals, we observed fine blood vessels of 100 μm or less.

1. Introduction

Synchrotrons generate monochromatic parallel x-ray beams using single crystals. These beams with photon energies of approximately 35 keV have been employed to perform enhanced K-edge angiography,[1-3] since the beams are absorbed effectively by iodine-based contrast media.

In order to perform high-speed medical radiography, although several different flash x-ray generators[4-9] utilizing cold-cathode tubes have been developed, plasma flash x-ray generators[10-13] are useful to produce quasi-monochromatic x rays without using a K-edge filter. Therefore, we have performed a demonstration of cone-beam K-edge angiography[14] utilizing a cerium plasma generator, since K-series characteristic x rays from the cerium target are absorbed effectively by iodine. Recently, we have developed a steady-state x-ray generator utilizing a cerium-target tube, and have demonstrated enhanced K-edge angiography utilizing a barium sulfate filter.[15] In this research, Kα lines (34.6 keV) were left by absorbing Kβ lines (39.2 keV).

In the present research, we describe a preliminary study on cone-beam K-edge angiography achieved with cerium Kα rays using a barium sulfate filter.

2. Generator

Figure 1 shows the block diagram of the x-ray generator, which consists of a main controller, a cerium-target x-ray tube unit with a Cockcroft-Walton circuit and an insulation transformer, and a personal computer. The tube voltage, the current, and the exposure time can be controlled by both the controller and the computer. The main circuit for producing x rays is illustrated in Fig. 2, and employs the Cockcroft-Walton circuit in order to decrease the dimensions of the tube unit. In the x-ray tube, the negative high-voltage is applied to the cathode electrode, and the anode (target) is connected to the tube unit case (ground potential) to cool the anode and the target effectively. The filament heating current is supplied by an AC power supply in the controller in conjunction with an insulation transformer. In this experiment, the tube voltage applied was from 45 to 65 kV, and the tube current was regulated to within 0.40 mA (maximum current) by the filament temperature. The exposure time is controlled in order to obtain optimum x-ray intensity. Monochromatic Kα lines were left using a 5-mm-thick barium sulfate filter in which barium sulfate powder was mixed with polymethyl methacrylate (PMMA) resin, since both the bremsstrahlung and the Kβ rays were absorbed effectively by the filter. In designing the filter, the surface density of the barium sulfate powder is important, since the x rays are absorbed effectively by the powder as compared with the PMMA resin. In this case, the density was approximately 10 mg/cm^2.

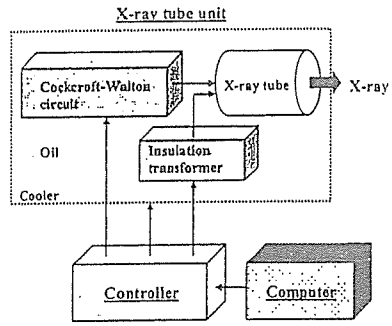

Fig. 1: Block diagram of compact x-ray generator with cerium-target tube.

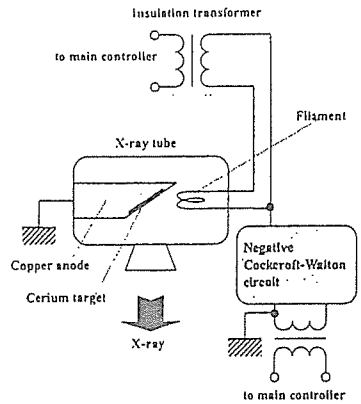

Fig. 2: Main circuit of x-ray generator.

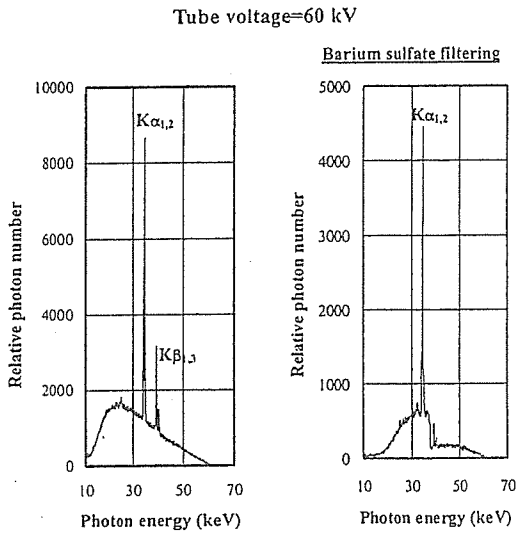

Fig. 3: X-ray spectra measured using germanium detector and filter.

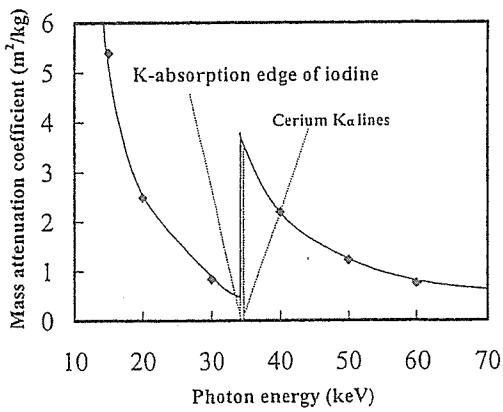

Fig. 4: Mass attenuation coefficients of iodine, and average photon energy of cerium Kα lines.

3. Characteristics

The x-ray intensity rate was measured by a Victoreen 660 ionization chamber at 1.0 m from the x-ray source. At a constant tube current of 0.40 mA, the x-ray intensity increased when the tube voltage was increased. In this measurement, the intensity with a tube voltage of 60 kV and a current of 0.40 mA was 16.8 μGy/s with errors of less than 0.2%.

In order to measure images of the x-ray source, we employed a pinhole camera with a hole diameter of 50 μm in conjunction with a Computed Radiography (CR) system[16] with a sampling pitch of 87.5 μm. When the tube voltage was increased, spot dimensions increased slightly and had values of

approximately 1×1 mm.

In order to measure x-ray spectra, we employed a germanium detector (GLP-10180/07-P, Ortec Inc.) (Fig. 3). When the tube voltage was increased, the Kα intensity substantially increased, and both the maximum photon energy and the intensities of bremsstrahlung x rays increased.

4. Angiography

Figure 4 shows the mass attenuation coefficients of iodine at the selected energies; the coefficient curve is discontinuous at the iodine K-edge. The average photon energy of the cerium Kα lines is shown just above the iodine K-edge. Cerium is a rare earth element and has a high reactivity; however, the average photon energies of Kα is 34.6 keV, and iodine contrast mediums with a K-absorption edge of 33.2 keV absorb the lines easily. Therefore, blood vessels were observed with high contrasts.

The angiography was performed using the CR system (Konica Regius 150), iodine microspheres of 15 μm in diameter, and the filter. The distance (between the x-ray source and the imaging plate) was 1.5 m, and the tube voltage was 60 kV. Figure 5 shows angiograms of an extracted dog heart. Because the size of the dog heart is almost the same as human heart, human coronary arteries can be observed.

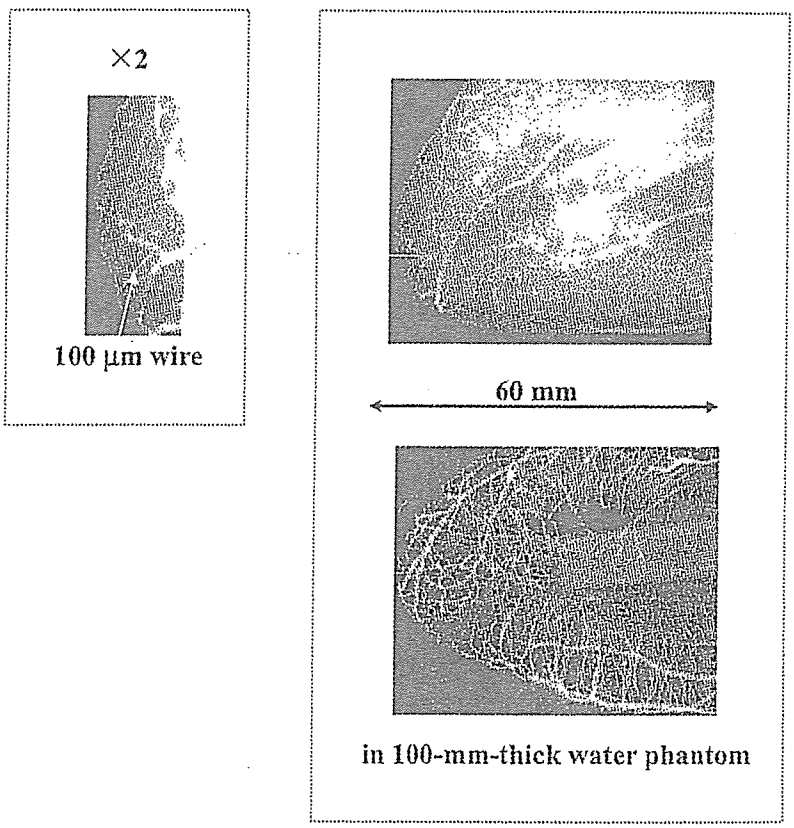

Fig. 5: Angiogram of extracted dog heart using iodine microspheres.

5. Discussion and Conclusions

In summary, we developed a new x-ray generator with a cerium-target tube and succeeded in producing cerium Kα lines, which can be absorbed easily by iodine-based contrast media. Both the characteristic and bremsstrahlung x-ray intensities increased with increases in the tube voltage, and Kβ lines were absorbed effectively by the barium sulfate filter.

In this preliminary experiment, although the maximum tube voltage and current were 65 kV and 0.40 mA, respectively, the voltage and current could be increased. Subsequently, the generator produced maximum number of Kα photons was approximately 3×10^7 photons/cm^2·s at 1.0 m from the source, and the photon count rate can be increased easily by improving the target.

Acknowledgment

This work was supported by Grants-in-Aid for Scientific Research (13470154, 13877114, and 16591222) and Advanced Medical Scientific Research from MECSST, Health and Labor Sciences Research Grants (RAMT-nano-001, RHGTEFB-genome-005 and RHGTEFB-saisei-003), Grants from Keiryo Research Foundation, The Promotion and Mutual Aid Corporation for Private Schools of Japan, Japan Science and Technology Agency (JST), and New Energy and Industrial Technology Development Organization (NEDO, Industrial Technology Research Grant Program in '03).

References

1. A. C. Thompson, H. D. Zeman, G. S. Brown, J. Morrison, P. Reiser, V. Padmanabahn, L. Ong, S. Green, J. Giacomini, H. Gordon and E. Rubenstein, "First operation of the medical research facility at the NSLS for coronary angiography," *Rev. Sci. Instrum.*, **63**, 625-628, 1992.

2. H. Mori, K. Hyodo, E. Tanaka, M. U. Mohammed, A. Yamakawa, Y. Shinozaki, H. Nakazawa, Y. Tanaka, T. Sekka, Y. Iwata, S. Honda, K. Umetani, H. Ueki, T. Yokoyama, K. Tanioka, M. Kubota, H. Hosaka, N. Ishizawa and M. Ando, "Small-vessel radiography in situ with monochromatic synchrotoron radiation," *Radiology*, **201**, 173-177, 1996.

3. K. Hyodo, M. Ando, Y. Oku, S. Yamamoto, T. Takeda, Y. Itai, S. Ohtsuka, Y. Sugishita and J. Tada, "Development of a two-dimensional imaging system for clinical applications of intravenous coronary angiography using intense synchrotron radiation produced by a multipole wiggler," *J. Synchrotron Rad.*, **5**, 1123-1126, 1998.

4. E. Sato, H. Isobe and F. Hoshino, "High intensity flash x-ray apparatus for biomedical radiography," *Rev. Sci. Instrum.*, **57**, 1399-1408, 1986.

5. E. Sato, S. Kimura, S. Kawasaki, H. Isobe, K. Takahashi, Y. Tamakawa and T. Yanagisawa, "Repetitive flash x-ray generator utilizing a simple diode with a new type of energy-selective function," *Rev. Sci. Instrum.*, **61**, 2343-2348, 1990.

6. A. Shikoda, E. Sato, M. Sagae, T. Oizumi, Y. Tamakawa and T. Yanagisawa, "Repetitive flash x-ray

generator having a high-durability diode driven by a two-cable-type line pulser," *Rev. Sci. Instrum.*, 65, 850-856, 1994.

7. E. Sato, K. Takahashi, M. Sagae, S. Kimura, T. Oizumi, Y. Hayasi, Y. Tamakawa and T. Yanagisawa, "Sub-kilohertz flash x-ray generator utilizing a glass-enclosed cold-cathode triode," *Med. & Biol. Eng. & Comput.*, **32**, 289-294, 1994.

8. E. Sato, M. Sagae, E. Tanaka, Y. Hayasi, R. Germer, H. Mori, T. Kawai, T. Ichimaru, S. Sato, K. Takayama and H. Ido, "Quasi-monochromatic flash x-ray generator utilizing a disk-cathode molybdenum tube," *Jpn. J. Appl. Phys.*, **43**, 7324-7328, 2004.

9. E. Sato, E. Tanaka, H. Mori, T. Kawai, T. Ichimaru, S. Sato, K. Takayama and H. Ido, "Compact monochromatic flash x-ray generator utilizing a disk-cathode molybdenum tube," *Med. Phys.*, **32**, 49-54, 2005.

10. E. Sato, Y. Hayasi, R. Germer, E. Tanaka, H. Mori, T. Kawai, H. Obara, T. Ichimaru, K. Takayama and H. Ido, "Irradiation of intense characteristic x-rays from weakly ionized linear molybdenum plasma," *Jpn. J. Med. Phys.*, **23**, 123-131, 2003.

11. E. Sato, Y. Hayasi, R. Germer, E. Tanaka, H. Mori, T. Kawai, T. Ichimaru, K. Takayama and H. Ido, "Quasi-monochromatic flash x-ray generator utilizing weakly ionized linear copper plasma," *Rev. Sci. Instrum.*, **74**, 5236-5240, 2003.

12. E. Sato, R. Germer, Y. Hayasi, Y. Koorikawa, K. Murakami, E. Tanaka, H. Mori, T. Kawai, T. Ichimaru, F. Obata, K. Takahashi, S. Sato, K. Takayama and H. Ido, "Weakly ionized plasma flash x-ray generator and its distinctive characteristics," *SPIE*, **5196**, 383-392, 2003.

13. E. Sato, Y. Hayasi, R. Germer, E. Tanaka, H. Mori, T. Kawai, T. Ichimaru, S. Sato, K. Takayama and H. Ido, "Sharp characteristic x-ray irradiation from weakly ionized linear plasma," *J. Electron Spectrosc. Related Phenom.*, **137-140**, 713-720, 2004.

14. E. Sato, R. Germer, Y. Hayasi, K. Murakami, Y. Koorikawa, E. Tanaka, H. Mori, T. Kawai, T. Ichimaru, F. Obata, K. Takahashi, S. Sato, K. Takayama and H. Ido, "Weakly ionized cerium plasma radiography," *SPIE*, **5210**, 12-21, 2003.

15. E. Sato, E. Tanaka, H. Mori, T. Kawai, T. Ichimaru, S. Sato, K. Takayama and H. Ido, "Demonstration of enhanced K-edge angiography using a cerium target x-ray generator," *Med. Phys.*, **31**, 3017-3021, 2004.

16. E. Sato, K. Sato and Y. Tamakawa, "Film-less computed radiography system for high-speed imaging," *Ann. Rep. Iwate Med. Univ. Sch. Lib. Arts and Sci.*, **35**, 13-23, 2000.

X-ray spectra from a cerium target and their application to cone beam K-edge angiography

Eiichi Sato, MEMBER SPIE
Iwate Medical University
Department of Physics
Morioka 020-0015, Japan
E-mail: dresato@iwate-med.ac.jp

Akira Yamadera
Hirosaki University
Department of Radiological Technology
School of Health Sciences
Hirosaki 036-8564, Japan

Etsuro Tanaka
Tokyo University of Agriculture
Department of Nutritional Science
Faculty of Applied Bioscience
Setagaya-ku 156-8502, Japan

Hidezo Mori
National Cardiovascular Center Research Institute
Department of Cardiac Physiology
Osaka 565-8565, Japan

Toshiaki Kawai, MEMBER SPIE
Hamamatsu Photonics K. K.
Electron Tube Division 2
Iwata 438-0193, Japan

Fumihito Ito
Digital Culture Technology Corporation
Kanno The 2nd Building.
Morioka 020-0021, Japan

Takashi Inoue
Akira Ogawa
Iwate Medical University
Department of Neurosurgery
School of Medicine
Morioka 020-8505, Japan

Shigehiro Sato
Iwate Medical University
Department of Microbiology
School of Medicine
Morioka 020-8505, Japan

Kazuyoshi Takayama, MEMBER SPIE
Tohoku University
Shock Wave Research Center
Institute of Fluid Science
Sendai 980-8577, Japan

Jun Onagawa
Hideaki Ido
Tohoku Gakuin University
Department of Applied Physics and Informatics
Faculty of Engineering
Tagajo 985-8537, Japan

0091-3286/2005/$22.00 © 2005 SPIE

Abstract. The cerium-target x-ray tube is useful for performing cone beam K-edge angiography, because K-series characteristic x-rays from the cerium target are absorbed effectively by iodine-based contrast media. The x-ray generator consists of a main controller and a unit with a high-voltage circuit and a fixed anode x-ray tube. The tube is a glass-enclosed diode with a cerium target and a 0.5-mm-thick beryllium window. The maximum tube voltage and current are 65 kV and 0.4 mA, respectively, and the focal-spot sizes are 1.3×0.9 mm. Cerium K-series characteristic x-rays are left, using a 3.0-mm-thick aluminum filter, and the x-ray intensity is 19.9 μGy/s at 1.0 m from the source with a tube voltage of 60 kV and a current of 0.40 mA. Angiography is performed with a computed radiography system using iodine-based microspheres 15 μm in diameter. In angiography of nonliving animals, we observe fine blood vessels of approximately 100 μm with high contrasts. © *2005 Society of Photo-Optical Instrumentation Engineers.* [DOI: 10.1117/1.2049268]

Subject terms: x-ray tube; cerium target; quasimonochromatic x-rays; characteristic x-rays; K-edge angiography.

Paper 040733R received Oct. 6, 2004; revised manuscript received Mar. 8, 2005; accepted for publication Mar. 11, 2005; published online Sep. 16, 2005. This paper is a revision of a paper presented at the SPIE conference on X-Ray Sources and Optics, August 2004, Denver, CO. The paper presented there appears (unrefereed) in SPIE Proceedings Vol. 5537.

1 Introduction

Monochromatic parallel x-ray beams are the basis of radiography using synchrotrons in conjunction with single crystals, and these beams have been employed to perform enhanced K-edge angiography[1–3] and x-ray phase imaging.[4–6] In angiography, the beams with photon energies of approximately 35 keV are absorbed effectively by iodine-based contrast media. However, it is difficult to obtain sufficient machine times for various research projects, including medical applications. Subsequently, monochromatic cone beams with energies of approximately 35 keV are useful for increasing the irradiation field for K-edge angiography.

To perform high-speed medical radiography, although several different flash x-ray generators[7–13] utilizing cold-cathode tubes have been developed, plasma flash x-ray generators[14–18] are useful for producing quasimonochromatic x-rays without using a K-edge filter. Therefore, we have performed a demonstration of cone beam K-edge

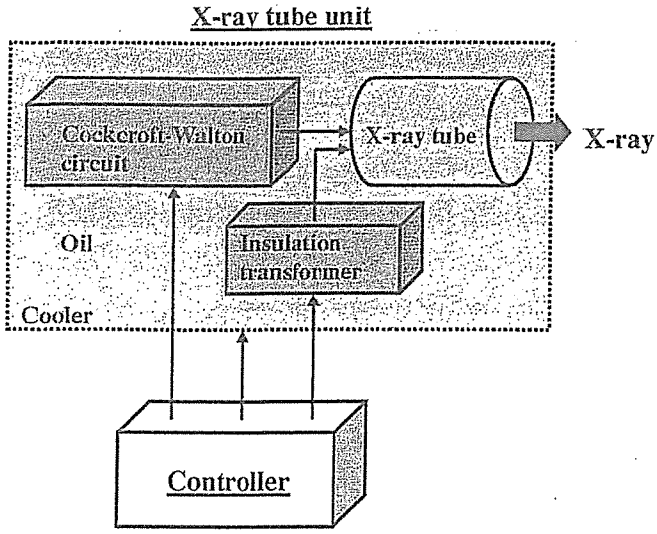

Fig. 1 Block diagram of the compact x-ray generator with a cerium-target radiation tube, which is used specially for K-edge angiography using iodine-based contrast media.

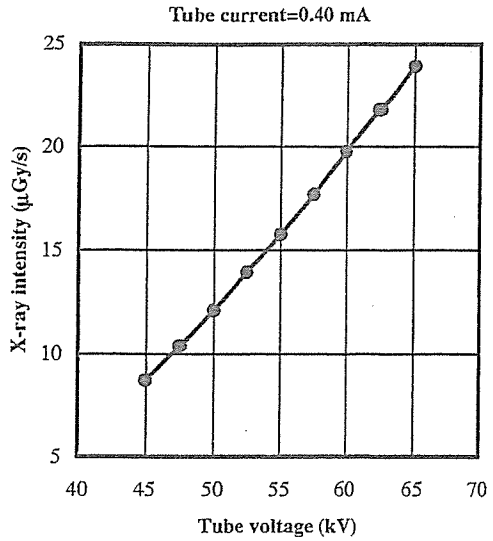

Fig. 3 The x-ray intensity (μGy/s) as a function of tube voltage (kV) with a tube current of 0.40 mA.

angiography[19] utilizing a cerium plasma generator, since K-series characteristic x-rays from the cerium target are absorbed effectively by iodine.

Recently, we have developed a steady-state x-ray generator utilizing a cerium-target tube, and have demonstrated enhanced K-edge angiography utilizing cerium Kα lines (34.6 keV).[20] In this research, Kα lines were left by absorbing Kβ lines (39.2 keV) using a barium sulfate filter with a barium K edge of 37.4 keV. However, because cerium Kβ lines are also absorbed effectively by iodine, both Kα and Kβ lines can be selected to increase the x-ray intensity for angiography. In measurements of x-ray spectra, although we usually employed a cadmium telluride detector with a photon energy resolution of 1.7 keV, the resolution should be minimized to measure the characteristic x-ray intensity.

In the present research, we measured the x-ray spectra from a cerium-target tube using a germanium detector, and performed a preliminary study on cone beam K-edge angiography achieved with cerium characteristic x-rays without using a K-edge filter.

2 Experimental Setup

Figure 1 shows the block diagram of the x-ray generator, which consists of a main controller and an x-ray tube unit with a Cockcroft-Walton circuit and a cerium-target tube. The tube voltage, the current, and the exposure time can be controlled by the controller. The main circuit for producing x-rays is illustrated in Fig. 2, and employs the Cockcroft-Walton circuit to decrease the dimensions of the tube unit. In the x-ray tube, the negative high voltage is applied to the cathode electrode, and the anode (target) is connected to the tube unit case (ground potential) to cool the anode and the target effectively. The filament heating current is supplied by an AC power supply in the controller in conjunction with an insulation transformer. In this experiment, the tube

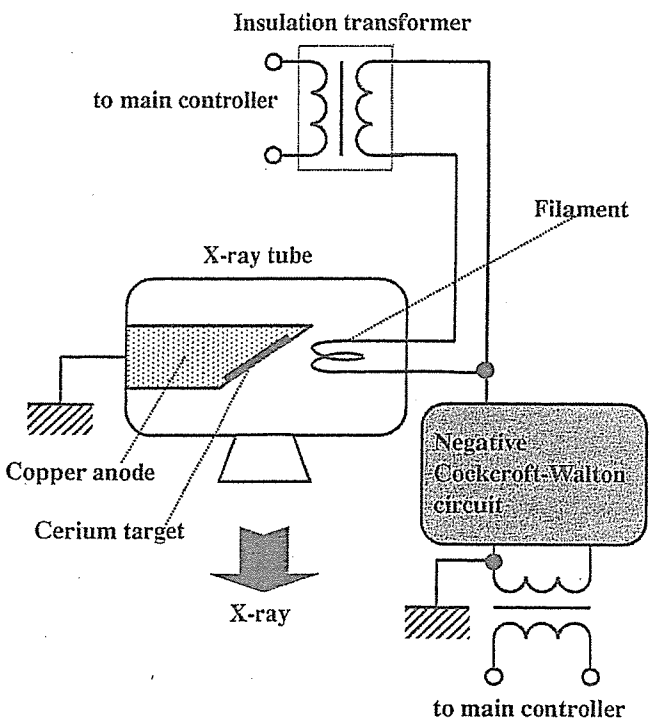

Fig. 2 Main circuit of the x-ray generator.

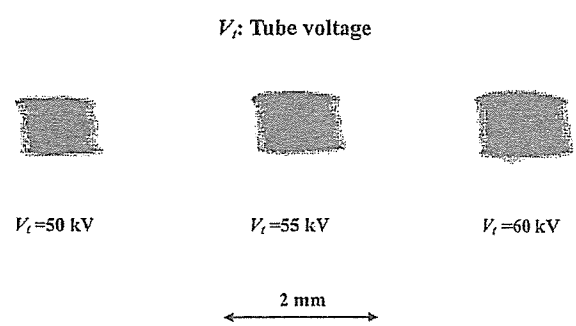

Fig. 4 Effective focal spots with changes in the tube voltage.

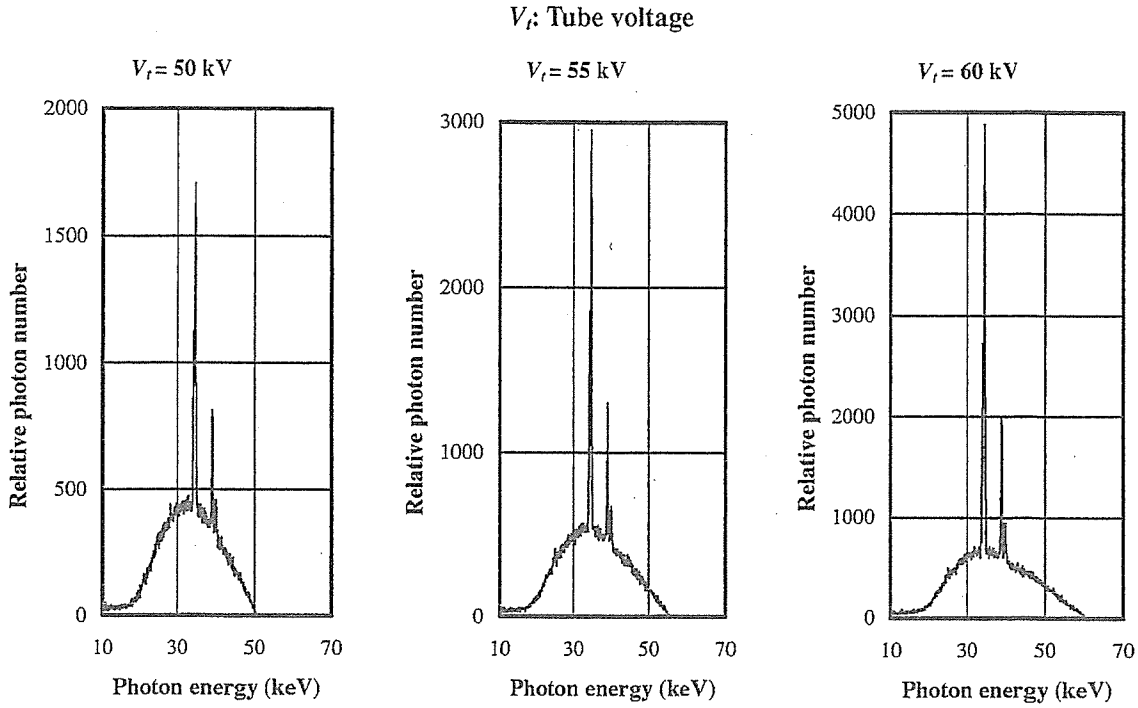

Fig. 5 X-ray spectra measured using a germanium detector with changes in the tube voltage.

voltage applied was from 45 to 65 kV, and the tube current was regulated to within 0.40 mA (maximum current) by the filament temperature. The exposure time is controlled to obtain optimum x-ray intensity. Quasimonochromatic x-rays are produced using a 3.0-mm-thick aluminum filter for absorbing soft bremsstrahlung rays.

3 Results and Discussion

3.1 *X-ray Intensity*

X-ray intensity was measured by a Victoreen 660 ionization chamber at 1.0 m from the x-ray source using the filter (Fig. 3). At a constant tube current of 0.40 mA, the x-ray intensity increased when the tube voltage was increased. In this measurement, the intensity with a tube voltage of 60 kV and a current of 0.40 mA was 19.9 μGy/s at 1.0 m from the source, with errors of less than 0.2%.

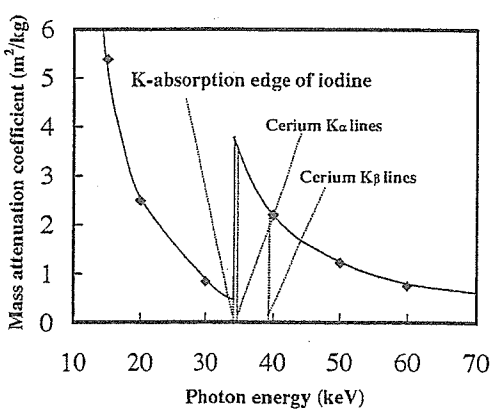

Fig. 6 Mass attenuation coefficients of iodine, and the average photon energies of cerium Kα and Kβ lines.

3.2 *Focal Spot*

To measure images of the x-ray source after the aluminum filtration, we employed a pinhole camera with a hole diameter of 50 μm (magnification ratio of 1:2) in conjunction with a computed radiography (CR) system[21] with a sampling pitch of 87.5 μm. When the tube voltage was increased, spot dimensions increased slightly and had values of 1.3 × 0.9 mm (Fig. 4).

3.3 *X-ray Spectra*

To measure x-ray spectra, we employed a germanium detector (GLP-10180/07-P, Ortec Incorporated) with a photon energy resolution of approximately 0.12 keV (Fig. 5). When the tube voltage was increased, the characteristic x-ray intensities of Kα and Kβ lines substantially increased, and both the maximum photon energy and the intensities of bremsstrahlung x-rays increased. Because the widths of the lines were approximately 1 keV, the photon energy resolution of this detector was an optimum value. In an empirical equation, because the characteristic x-ray in-

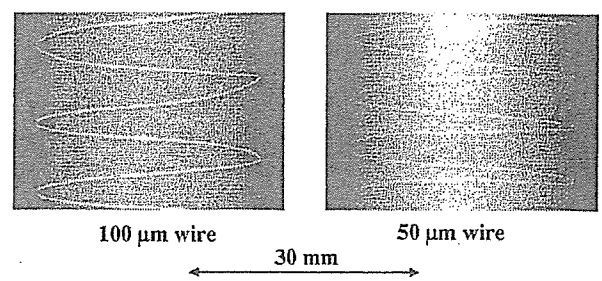

Fig. 7 Radiograms of tungsten wires coiled around PMMA rods with a tube voltage of 60 kV.

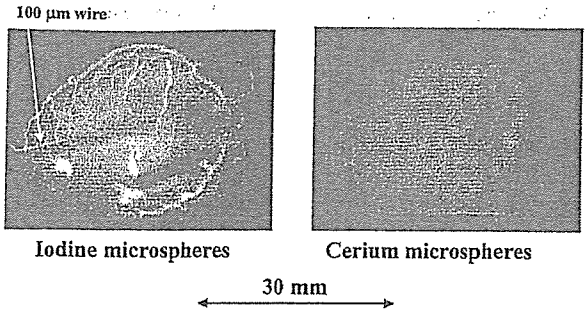

Fig. 8 Angiograms of extracted rabbit hearts using iodine and cerium microspheres with a tube voltage of 60 kV.

tensity is proportional to approximately 1.5 power of the voltage difference between the tube voltage and the critical excitation voltage, the measured intensities of the characteristic x-rays corresponded well to the equation.

3.4 *K-Edge Angiography*

Figure 6 shows the mass attenuation coefficients of iodine at the selected energies; the coefficient curve is discontinuous at the iodine K edge. The average photon energy of the cerium Kα and Kβ lines are shown just above the iodine K edge. The average photon energies of Kα and Kβ lines are 34.6 and 39.2 keV, respectively, and iodine contrast media with a K-absorption edge of 33.2 keV absorb the lines easily. Therefore, blood vessels were observed with high contrasts.

The angiography was performed by a CR system (Konica Minolta Regius 150) using the filter, and the distance (between the x-ray source and the imaging plate) was 1.5 m. First, rough measurements of spatial resolution were made using wires. Figure 7 shows radiograms of tungsten wires coiled around a rod made of polymethyl methacrylate. Although the image contrast decreased somewhat with decreases in the wire diameter, due to blurring of the image caused by the sampling pitch of 87.5 μm, a 50-μm-diam wire could be observed.

Angiograms of rabbit hearts are shown in Fig. 8. These two images were obtained using iodine and cerium microspheres of 15 μm in diameter at a tube voltage of 60 kV.

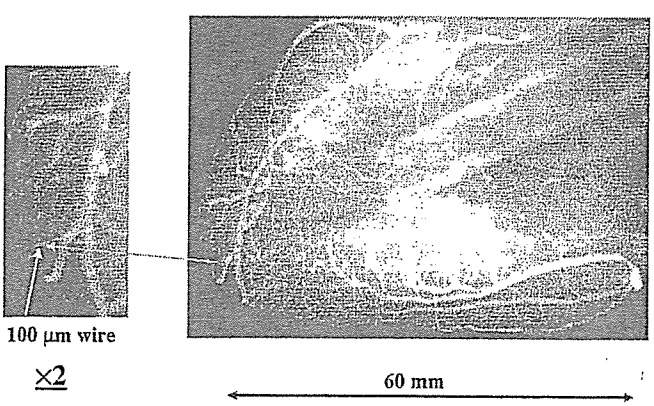

Fig. 9 Angiograms of an extracted dog heart using iodine microspheres with a tube voltage of 60 kV.

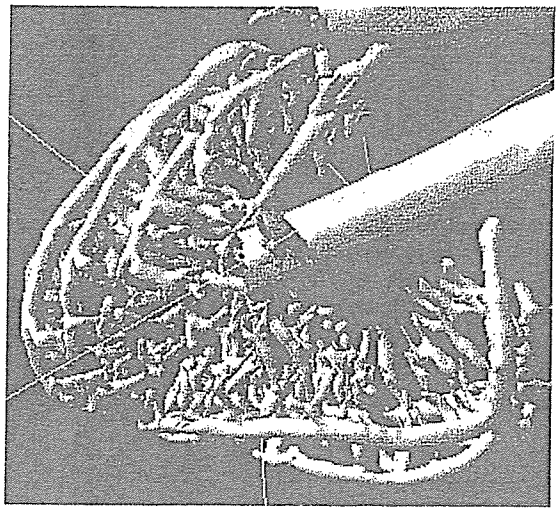

Fig. 10 3-D image of coronary arteries constructed from x-ray CT images by Pascal.

The microspheres are very useful for making phantoms of nonliving animals used for angiography. The iodine plastic spheres contained 37% iodine by weight, and the cerium plastic spheres were chemically stable and contained 18% cerium by weight. In the case where the cerium spheres were employed, the coronary arteries were barely visible, since the cerium spheres transmitted cerium characteristic x-rays easily. Figure 9 shows an angiogram of a larger dog heart at a tube voltage of 60 kV using iodine spheres. For comparison, we show a 3-D image of the coronary arteries constructed from x-ray CT images by Pascal (Digital Culture Technical Corporation) with a tungsten x-ray tube (Fig. 10). Using this imaging technique, fine blood vessels were not observed at all.

4 Conclusion and Outlook

In summary, we employ an x-ray generator with a cerium-target tube and succeed in producing cerium characteristic x-rays, which can be absorbed easily by iodine-based contrast media. The characteristic x-ray intensities increase with increases in the tube voltage, and low-photon-energy bremsstrahlung rays are absorbed effectively by the filter.

Although the cerium x-ray generator used in this research produces both the characteristic and the bremsstrahlung x-rays, bremsstrahlung intensity can be decreased effectively by considering the angle dependence without using the filter, since bremsstrahlung rays are not emitted in the opposite direction to that of electron trajectory in Sommerfeld's theory.[22] Subsequently, the generator-produced maximum number of characteristic photons is approximately 3.5×10^7 photons/cm$^2 \cdot$s at 1.0 m from the source, and the photon count rate can be increased easily by improving the target.

The x-ray intensity is limited because the thermal contact between the target and the anode is not good. However, the intensity can be increased by welding the target or using a cerium-alloy target. In addition, a rotation anode tube can be developed by the sputtering of cerium.

Compared to the 3-D blood images constructed from x-ray CT images by Pascal, fine blood vessels are visible.

Because the sampling pitch of the CR system is 87.5 μm, we obtain spatial resolutions of approximately 100 μm. To observe fine blood vessels of less than 100 μm, the spatial resolution of the CR system should be improved to approximately 50 μm (Konica Minolta Regius 190). In addition, the spatial resolution can be improved easily to approximately 50 μm or less in cases where an x-ray film (Fuji Ix 100) is employed.

Acknowledgment

This work was supported by Grants-in-Aid for Scientific Research (13470154, 13877114, and 16591222) and Advanced Medical Scientific Research from MECSST, Health and Labor Sciences Research Grants (RAMT-nano-001, RHGTEFB-genome-005, and RHGTEFB-saisei-003), grants from Keiryo Research Foundation, The Promotion and Mutual Aid Corporation for Private Schools of Japan, Japan Science and Technology Agency (JST), and New Energy and Industrial Technology Development Organization (NEDO, Industrial Technology Research Grant Program in 2003).

References

1. A. C. Thompson, H. D. Zeman, G. S. Brown, J. Morrison, P. Reiser, V. Padmanabahn, L. Ong, S. Green, J. Giacomini, H. Gordon, and E. Rubenstein, "First operation of the medical research facility at the NSLS for coronary angiography," *Rev. Sci. Instrum.* **63**, 625–628 (1992).
2. H. Mori, K. Hyodo, E. Tanaka, M. U. Mohammed, A. Yamakawa, Y. Shinozaki, H. Nakazawa, Y. Tanaka, T. Sekka, Y. Iwata, S. Honda, K. Umetani, H. Ueki, T. Yokoyama, K. Tanioka, M. Kubota, H. Hosaka, N. Ishizawa, and M. Ando, "Small-vessel radiography in situ with monochromatic synchrotoron radiation," *Radiology* **201**, 173–177 (1996).
3. K. Hyodo, M. Ando, Y. Oku, S. Yamamoto, T. Takeda, Y. Itai, S. Ohtsuka, Y. Sugishita, and J. Tada, "Development of a two-dimensional imaging system for clinical applications of intravenous coronary angiography using intense synchrotron radiation produced by a multipole wiggler," *J. Synchrotron Radiat.* **5**, 1123–1126 (1998).
4. T. J. Davis, D. Gao, T. E. Gureyev, A. W. Stevenson, and S. W. Wilkims, "Phase-contrast imaging of weakly absorbing materials using hard x-rays," *Nature (London)* **373**, 595–597 (1995).
5. A. Momose, T. Takeda, Y. Itai, and K. Hirano, "Phase-contrast x-ray computed tomography for observing biological soft tissues," *Nat. Med.* **2**, 473–475 (1996).
6. M. Ando, A. Maksimenko, H. Sugiyama, W. Pattanasiriwisawa, K. Hyodo, and C. Uyama, "A simple x-ray dark- and bright-field imaging using achromatic Laue optics," *Jpn. J. Appl. Phys., Part 2* **41**, L1016–L1018 (2002).
7. E. Sato, S. Kimura, S. Kawasaki, H. Isobe, K. Takahashi, Y. Tamakawa, and T. Yanagisawa, "Repetitive flash x-ray generator utilizing a simple diode with a new type of energy-selective function," *Rev. Sci. Instrum.* **61**, 2343–2348 (1990).
8. E. Sato, M. Sagae, K. Takahashi, T. Oizumi, H. Ojima, K. Takayama, Y. Tamakawa, T. Yanagisawa, A. Fujiwara, and K. Mitoya, "High-speed soft x-ray generators in biomedicine," *Proc. SPIE* **2513**, 649–667 (1994).
9. E. Sato, M. Sagae, K. Takahashi, A. Shikoda, T. Oizumi, H. Ojima, K. Takayama, Y. Tamakawa, T. Yanagisawa, A. Fujiwara, and K. Mitoya, "Dual energy flash x-ray generator," *Proc. SPIE* **2513**, 723–735 (1994).
10. A. Shikoda, E. Sato, M. Sagae, T. Oizumi, Y. Tamakawa, and T. Yanagisawa, "Repetitive flash x-ray generator having a high-durability diode driven by a two-cable-type line pulser," *Rev. Sci. Instrum.* **65**, 850–856 (1994).
11. E. Sato, K. Takahashi, M. Sagae, S. Kimura, T. Oizumi, Y. Hayasi, Y. Tamakawa, and T. Yanagisawa, "Sub-kilohertz flash x-ray generator utilizing a glass-enclosed cold-cathode triode," *Med. Biol. Eng. Comput.* **32**, 289–294 (1994).
12. K. Takahashi, E. Sato, M. Sagae, T. Oizumi, Y. Tamakawa, and T. Yanagisawa, "Fundamental study on a long-duration flash x-ray generator with a surface-discharge triode," *Jpn. J. Appl. Phys., Part 1* **33**, 4146–4151 (1994).
13. E. Sato, M. Sagae, A. Shikoda, K. Takahashi, T. Oizumi, M. Yamamoto, A. Takabe, K. Sakamaki, Y. Hayasi, H. Ojima, K. Takayama, and Y. Tamakawa, "High-speed soft x-ray techniques," *Proc. SPIE* **2869**, 937–955 (1996).
14. E. Sato, Y. Hayasi, E. Tanaka, H. Mori, T. Kawai, T. Usuki, K. Sato, H. Obara, T. Ichimaru, K. Takayama, H. Ido, and Y. Tamakawa, "Quasi-monochromatic radiography using a high-intensity quasi-x-ray laser generator," *Proc. SPIE* **4682**, 538–548 (2002).
15. E. Sato, Y. Hayasi, R. Germer, E. Tanaka, H. Mori, T. Kawai, H. Obara, T. Ichimaru, K. Takayama, and H. Ido, "Intense characteristic x-ray irradiation from weakly ionized linear plasma and applications," *Jpn. J. Med. Imag. Inform. Sci.* **20**, 148–155 (2003).
16. E. Sato, Y. Hayasi, R. Germer, E. Tanaka, H. Mori, T. Kawai, H. Obara, T. Ichimaru, K. Takayama, and H. Ido, "Irradiation of intense characteristic x-rays from weakly ionized linear molybdenum plasma," *Jpn. J. Med. Phys.* **23**, 123–131 (2003).
17. E. Sato, Y. Hayasi, R. Germer, E. Tanaka, H. Mori, T. Kawai, T. Ichimaru, K. Takayama, and H. Ido, "Quasi-monochromatic flash x-ray generator utilizing weakly ionized linear copper plasma," *Rev. Sci. Instrum.* **74**, 5236–5240 (2003).
18. E. Sato, Y. Hayasi, R. Germer, E. Tanaka, H. Mori, T. Kawai, T. Ichimaru, S. Sato, K. Takayama, and H. Ido, "Sharp characteristic x-ray irradiation from weakly ionized linear plasma," *J. Electron Spectrosc. Relat. Phenom.* **137-140**, 713–720 (2004).
19. E. Sato, R. Germer, Y. Hayasi, K. Murakami, Y. Koorikawa, E. Tanaka, H. Mori, T. Kawai, T. Ichimaru, F. Obata, K. Takahashi, S. Sato, K. Takayama, and H. Ido, "Weakly ionized cerium plasma radiography," *Proc. SPIE* **5210**, 12–21 (2003).
20. E. Sato, E. Tanaka, H. Mori, T. Kawai, T. Ichimaru, S. Sato, K. Takayama, and H. Ido, "Demonstration of enhanced K-edge angiography using a cerium target x-ray generator," *Med. Phys.* **31**, 3017 (2004).
21. E. Sato, K. Sato, and Y. Tamakawa, "Film-less computed radiography system for high-speed imaging," *Ann. Rep. Iwate Med. Univ. Sch. Lib. Arts Sci.* **35**, 13–23 (2000).
22. B. K. Agarwal, *X-Ray Spectroscopy*, 2nd ed., p. 18, Springer-Verlag, New York (1991).

Eiichi Sato received his BS, MS, and PhD in applied physics from Tohoku Gakuin University, Sendai, Japan, in 1979, 1982, and 1987, respectively. He is currently a professor in the Department of Physics at Iwate Medical University. He has written approximately 400 publications and delivered 200 international presentations concerning x-rays. His research interests include soft flash x-ray generators, quasi-x-ray laser generators, and high-speed radiography. In 2000, he received the Schardin Gold Medal from the German Physical Society, in 2003 he received the Takayama Award (Gold Medal) from the Japan Society of High Speed Photography and Photonics, and he received the Honorable Mention Poster Award from the SPIE International Symposium on Medical Imaging 2005.

Akira Yamadera received his BS, MS, and PhD degrees in physics from Tohoku University in 1969, 1971, and 1978, respectively. He is currently a professor in the Department of Radiological Technology, School of Health Sciences at Hirosaki University. His research interests include radiation dose measurement using imaging plates, radiation safety, environmental radiation measurements, and x-ray spectroscopy.

Etsuro Tanaka received his MD and PhD degrees in medicine from Kumamoto University, Japan, in 1980 and 1986, respectively. He worked on medical image processing in the Department of Physiology, Tokai University, Japan, from 1988 to 2003. He is currently a professor in the Department of Nutritional Sciences, Tokyo University of Agriculture, Japan. His research interests include medical image processing, human physiology, and clinical nutrition.

Hidezo Mori received a medical degree from Keio University School of Medicine, Tokyo, Japan, in 1977, and also a PhD from the Post Graduate School, Keio University School of Medicine. Now he is the director of the Department of Cardiac Physiology at the National Cardiovascular Center, Suita, Japan. His primary research interests are regenerative therapy in cardiovascular disease, microcirculation, and medical applications of structural biology.

Toshiaki Kawai received the BS degree in precision mechanics and the MS degree in electronic engineering from Shizuoka University, Hamamatsu, Japan, in 1964 and 1974, respectively. In 1974, he joined the Hamamatsu Photonics K.K., where he worked on research and development of solid-state infrared detectors, and then from 1978 to 1981 engaged in research work on the NEA cold cathode for application to imaging camera tubes. He is now the project coordinator of Electron Tube Division 2 and is engaged in the development and manufacturing of imaging devices and x-ray equipment. He is a member of the Japan Radioisotope Association and the Institute of Image Information and Television Engineers of Japan.

Fumihito Ito left the Department of Mechanical Engineering, Iwate University, in 2001. Since 2002, he has been a member of the research and development section of the Digital Culture Technology Corporation, Japan. Since 2004 he has been a student on the doctoral course in the Faculty of Software and Information Science at Iwate Prefectural University. His research interests include 3-D imaging reconstructed from images in optical coherence tomography (OCT), x-ray CT, and MRI.

Takashi Inoue received his MD and PhD degrees in 2000 from Tohoku University. He is currently an assistant professor in the Department of Neurosurgery at Iwate Medical University, and a member of the Japan Neurosurgical Society. His research interests include neurosurgery and MRI.

Akira Ogawa received his MD and PhD degrees in 1981 from Tohoku University. He is currently a professor in the Department of Neurosurgery and Dean of the School of Medicine at Iwate Medical University, and is a trustee of the Japan Neurosurgical Society. His research interests include neurosurgery and cerebrovascular disease.

Shigehiro Sato received his MD degree from Iwate Medical University in 1980. He worked for the laboratory of the Division of Pediatric Infectious Diseases at Johns Hopkins Hospital from 1985 to 1989. He is currently a professor in the Department of Microbiology at Iwate Medical University. His research interests include central nervous system damage caused by Vero toxin, a cell culture system for vaccine development, and microangiography.

Kazuyoshi Takayama received his BS degree from Nagoya Institute of Technology in 1962. In 1970, he received his PhD in mechanical engineering from Tohoku University. He is currently a director (professor) in the Shock Wave Research Center, Institute of Fluid Science at Tohoku University. His research interests include various shock wave phenomena, high speed photography, and flash radiography. He has received seven awards, including the coveted Ernst Mach Medal in 2000.

Jun Onagawa received his BS and PhD degrees in physics from Tohoku Gakuin University in 1968 and 2001, respectively. He is currently a professor in the Department of Applied Physics and Informatics, Faculty of Engineering, at Tohoku Gakuin University. His research interests include target metallography and x-ray spectroscopy.

Hideaki Ido received his BS, MS, and PhD degrees in physics from Tohoku University in 1962, 1964, and 1967, respectively. He is currently a professor in the Department of Applied Physics and Informatics, Faculty of Engineering, at Tohoku Gakuin University. His research interests include magnetism and x-ray spectroscopy.

Clinical and Experimental Pharmacology and Physiology (2005) **32**, 952–959

EXOGENOUS NITRIC OXIDE CENTRALLY ENHANCES PULMONARY REACTIVITY IN THE NORMAL AND HYPERTENSIVE RAT

Daryl O Schwenke,* James T Pearson,* Hirotsugu Tsuchimochi,* Hidezo Mori* and Mikiyasu Shirai†

**Department of Cardiac Physiology, National Cardiovascular Center Research Institute, Suita, Osaka and* †*Faculty of Health Sciences, Hiroshima International University, Hiroshima, Japan*

SUMMARY

1. Chronic hypoxia causes sustained pulmonary hypertension and, although impairment of the pulmonary endothelial nitric oxide (NO) pathway has been implicated, no study has described the central role of NO in modulating pulmonary vascular tone and reactivity. Centrally, NO inhibits sympathetic outflow, so we hypothesised that central NO would modulate pulmonary vascular tone and its reactivity to acute hypoxia, especially in the hypertensive state.

2. Male adult Sprague-Dawley rats were exposed to normoxia (N) or chronic hypoxia (CH; 12% O_2) for 14 days. Mean pulmonary arterial pressure (MPAP), systemic mean arterial blood pressure (MABP), cardiac output and heart rate were then measured in pentobarbitone-anaesthetized, artificially ventilated rats. The N and CH rats were exposed to acute hypoxia (10% O_2 for 4 min) after the intracerebroventricular (i.c.v.) administration of artificial cerebrospinal fluid (control) and then again after either i.c.v. N^G-nitro-L-arginine methyl ester (L-NAME; 150 μg in 10 μL) or 3-morpholino-sydnonimine hydrochloride (SIN-1; 100 μg in 10 μL).

3. Chronic hypoxia caused pulmonary hypertension (MPAP 20 ± 1 *vs* 30 ± 1 mmHg in N and CH rats, respectively) and attenuated acute hypoxic pulmonary vasoconstriction (HPV). Central inhibition of NO synthesis (by L-NAME) did not alter baseline MPAP or the acute HPV in either N or CH rats, but it did elevate MABP. The NO donor SIN-1 did not alter baseline MPAP, but it did enhance (N rats) or restore (CH rats) the HPV and decreased MABP.

4. The results of the present study indicate that central NO has a limited role in the tonic modulation of MPAP during normoxia and after chronic hypoxia. However, the acute HPV seems to be enhanced by exogenous NO.

Key words: chronic hypoxia, nitric oxide, pulmonary vasoconstriction, sympathetic nervous system.

INTRODUCTION

Acute alveolar hypoxia causes pulmonary vasoconstriction that is reversible upon re-oxygenation. However, during chronic hypoxia, as is the case with several chronic pulmonary pathological conditions, elevated shear stress within the pulmonary vasculature causes endothelial cell injury/dysfunction,[1] smooth muscle cell proliferation[2] and, inevitably, the irreversible remodelling of the pulmonary vasculature.[3,4] The consequential sustained increase in pulmonary arterial pressure (PAP) increases the workload of the heart and is therefore closely associated with heart failure and increased mortality.

Although the exact cellular mechanisms responsible for the pathogenesis of chronic hypoxia-induced pulmonary arterial hypertension are unknown, alterations in the endothelial nitric oxide (NO) pathway have been implicated as a significant contributing factor.[5,6] Nitric oxide is a potent vasodilator and an inhibitor of vascular remodelling.[7–9] Nitric oxide is produced from L-arginine in a reaction catalysed by isoenzymes of NO synthase (NOS). The synthesis of NO is blocked by several L-arginine analogues, including N^G-nitro-L-arginine methyl ester (L-NAME), which competitively and stereoselectively inhibit the generation of NO from L-arginine.[10]

A reduction in the production of NO has been implicated in the pathophysiology of pulmonary hypertension.[6,8] Endothelial NOS (eNOS)-knockout mice have an increased risk of pulmonary hypertension,[11–13] whereas the hypoxia-induced pulmonary hypertension is attenuated in transgenic mice that overexpress eNOS.[14] In addition, chronic hypoxia limits endogenous NO synthesis,[15] despite an increase in NOS expression.[16–18]

Nitric oxide is produced not only peripherally, but also centrally within various parts of the brain, including the nucleus tractus solitarius (NTS) of the medulla oblongata and the ventrolateral medulla, the cardiovascular regulatory centres.[19–21] Therefore, NO is considered to be involved in the neural regulation of blood pressure, independent of its direct effects on the endothelium of blood vessels.[22] A review by Patel *et al.*[23] reported that the general consensus in the literature was that NO acts as a sympatho-inhibitory substance within the central nervous system. Therefore, central NO inhibition increases sympathetic outflow and, subsequently, arterial blood pressure.[24,25]

The central role of NO in modulating pulmonary vasculature, especially in pathological conditions (e.g. pulmonary hypertension), is still incompletely understood. Yet, as evidence accumulates in support of central NO as an important regulator

Correspondence: Daryl O Schwenke, Department of Cardiac Physiology, National Cardiovascular Center Research Institute, 5-7-1 Fujishirodai, Suita, Osaka 565-8565, Japan. Email: schwenke@ri.ncvc.go.jp

Received 2 March 2005; revision 1 June 2005; accepted 17 July 2005.

of cardiovascular function, the central role of NO in the modulation of the pulmonary vasculature needs to be addressed. Therefore, our first aim in the present study was to elucidate the role of NO in the central modulation of pulmonary vascular tone under normoxic conditions and after the development of chronic hypoxia-induced pulmonary hypertension. Nitric oxide is thought to have an important role in modulating the hypoxic pulmonary vasoconstriction (HPV) in response to acute hypoxic challenges.[26] However, there are conflicting reports as to whether the HPV response is accentuated or attenuated by pulmonary hypertension.[6,27] Therefore, a second aim of the present study was to assess the acute HPV before and after chronic hypoxia and to determine whether central NO has a role in modulating this response.

METHODS

Animals

Experiments were conducted on 23 male Sprague-Dawley rats (8 weeks old; bodyweight approximately 200–280 g). Rats were divided into four groups, as follows: (i) group 1, normoxia (N) + L-NAME; (ii) group 2, chronic hypoxia (CH) + L-NAME; (iii) group 3, N + 3-morpholino-sydnonimine hydrochloride (SIN-1); and (iv) group 4, CH + SIN-1. The CH rats were housed in a hypoxic chamber (12.0 ± 0.1% O_2) continuously for 2 weeks, except for a 10 min interval each day when the chamber was cleaned. The N rats were housed in similar housing, except that N rats breathed room air. The hypoxic gas mixture was delivered to the hypoxic chamber (30 L capacity) at a flow rate of approximately 8 L/min. All rats were on a 12 h light/dark cycle at 25 ± 1°C and were provided with food and water *ad libitum*. All experiments were approved by the local Animal Ethics Committee and conducted in accordance with the guidelines of the Physiological Society of Japan (http://www.soc.nii.ac.jp/psj/).

Anaesthesia and surgery

Rats were initially anaesthetized with pentobarbitone sodium (45 mg/kg, i.p.) and supplementary doses of anaesthetic were administered periodically throughout the experimental protocol (15–30 mg/kg per h, i.p.) so as to maintain a constant surgical level of anaesthesia (assessed by using the limb withdrawal reflex test). Rectal temperature was maintained at 38°C using a rectal thermistor coupled to a thermostatically controlled heating pad.

Using a stereotaxic frame, the tip of a 27 gauge stainless steel cannula was positioned in the right lateral cerebral ventricle based on the coordinates of Paxinos and Watson[28] (0.8 mm posterior to the bregma, 1.5 mm lateral to the midline and 5.0 mm ventral to the skull surface). The distal end of the cannula was connected to a 0.5 mL syringe for subsequent drug administration. Correct positioning of the intracerebroventricular (i.c.v.) catheter was confirmed after each experiment by staining with Evans blue dye (10 μL).

The trachea was cannulated and the lungs ventilated with a rodent ventilator (SN-480-7; Shinano, Tokyo, Japan). The inspirate gas was enriched with O_2 (approximately 50% O_2) and the ventilator settings were adjusted (tidal volume (V_T) approximately 3.5 mL; frequency approximately 80 /min) to maintain arterial P_{CO_2} normocapnic. The femoral artery and vein were cannulated for the measurement of systemic arterial blood pressure and drug administration, respectively. The arterial line contained heparinized saline (50 U/mL). A right thoracotomy was made between the second and third ribs and the conus of the right ventricle was exposed. A 23 gauge needle was used to pierce the ventricle wall and then the gel-filled sensing catheter of a telemetric transmitter (model TA11PA-C40; Data Sciences, St Paul, MN, USA) was inserted anteriorly into the right ventricle and advanced into the pulmonary artery. The catheter was fixed in position with a 7.0 Prolene suture to the pericardium. The aorta was blunt dissected free from the pulmonary artery and a transonic perivascular flowprobe (model 2RB; Transonic Systems, Ithaca, NY, USA) was positioned around the ascending aorta for the continuous measurement of cardiac output.

Drugs

Artificial cerebrospinal fluid (aCSF) was used as the vehicle for administering the NOS inhibitor L-NAME and the slow-releasing NO donor, 3-[4-morpholinyl]-sydnonimine-hydrochloride (SIN-1). The aCSF (pH 7.36–7.43) was comprised of 150 mmol/L NaCl, 3.0 mmol/L KCl, 0.8 mmol/L $MgCl_2$, 1.4 mmol/L $CaCl_2$ and 1.0 mmol/L Na phosphate. Intracerebroventricular injections were given as a 10 μL bolus over 30 s. Intravenous (i.v.) injections were administered as a 0.2 mL bolus over 15 s, followed by a 0.1 mL saline flush.

Measurement of right ventricular weight

Immediately following the experiment, rats were killed by anaesthetic overdose, the heart was excised, the atria were removed and the right ventricle wall was separated from the left ventricle, including the septum. Tissues were blotted and weighed. Right and left ventricular weights were expressed as the ratio of the right ventricle to the left ventricular + septum weight ($W_{RV}/W_{LV+septum}$; Fulton's ratio).

Experimental protocols

Once all variables had stabilized after surgery (approximately 20 min), baseline values were recorded for 10 min in response to the i.c.v. administration of aCSF (10 μL). The inspirate was then switched to hypoxia (10% O_2 balanced by N_2) for 4 min. Upon recovery from acute hypoxia, rats received a bolus i.c.v. injection of either L-NAME (150 μg; groups 1 and 2) or SIN-1 (100 μg; groups 3 and 4). After 5 (L-NAME) or 10 min (SIN-1), the acute hypoxic test was repeated. After a further 10 min, once variables had recovered to prehypoxic values, rats (groups 1 and 2 only) received a bolus i.v. injection of L-NAME (50 mg/kg) and acute hypoxia was tested 10 min later.

Data acquisition and analysis

Pulmonary arterial pressure was measured using telemetry. The signal from the implanted transmitter (model TA11PA-C20; Data Sciences) was calibrated in reference to an input from an ambient-pressure monitor (C11PR; Data Sciences) and subsequently relayed to a personal computer. Cardiac output (CO) was measured continuously from the ascending aorta using a Transonic small animal blood flowmeter (model T206; Transonic Systems) with a flowprobe (model 2RB). Arterial blood pressure (ABP) was measured continuously with a Deltran pressure transducer (Utah Medical Products, Midvale, UT, USA) and the signal was relayed to a Powerlab bridge amplifier (ML117; ADInstruments, Tokyo, Japan).

The signals for ABP, CO and PAP were relayed from their respective units and sampled continuously at 200 Hz with an eight-channel MacLab/8s interface hardware system (ADInstruments) and recorded on a Macintosh Power Book G4 using Chart (v. 5.0.1; ADInstruments). Heart rate (HR) was derived from the arterial systolic peaks. Cardiac output was normalized (off-line) to 100 g bodyweight. Total systemic vascular resistance (SVR) and total pulmonary vascular resistance (PVR) were calculated by dividing mean ABP (MABP) and mean PAP (MPAP) by the normalized CO. A 10 block of data was analysed –60, –30 s and immediately before (time '0') acute hypoxic exposure and then after 20, 40, 60, 90, 120, 180 and 240 s of exposure to 10% O_2. Normoxic data for individual rats in each group were averaged from values acquired at –60, –30 s and at time 0. An arterial blood sample (0.1 mL) was extracted 5 min after the completion of surgery for analysis of arterial P_{CO_2} using an ABL 605 blood gas analyser (Radiometer, Copenhagen, Denmark). An additional 0.1 mL was extracted to measure haematocrit.

Statistical analysis

All statistical analyses were conducted using Statview (v. 5.01; SAS Institute, Cary, NC, USA). All results are presented as the mean±SEM. Two-way ANOVA (repeated measures) was used to test significance for: (i) changes in each variable in response to 4 min of acute hypoxia; and (ii) whether the hypoxic response was altered by drug administration (i.c.v. or i.v.).

One-way ANOVA (factorial) was used to test for differences in baseline values for normoxic and chronic hypoxic groups of rats. Where statistical significance was reached, post hoc analyses were incorporated using the paired or unpaired *t*-test with Dunnet's correction for multiple comparisons. $P \leq 0.05$ was predetermined as the level of significance for all statistical analyses.

RESULTS

Chronic hypoxia induced pulmonary hypertension (Table 1), as evidenced by the observation that the MPAP and PVR of CH rats ($n = 11$) was 50 and 34% higher, respectively, than that of normoxic (N) rats ($n = 12$; $P < 0.01$). Consequently, CH rats developed right ventricular hypertrophy (ΔRV/LV + Sep ratio of 0.23). Chronic hypoxia did not significantly change MABP or CO, but it did cause a significant reduction in HR (ΔHR 37 b.p.m.; $P < 0.01$), suggesting that the development of right ventricular hypertrophy resulted in an increase in stroke volume. An increase in haematocrit (ΔHct 18%; $P < 0.001$) also occurred in CH.

Responses to acute hypoxia

In N rats, acute exposure to 10% O_2 provoked an increase in MPAP, after a latency of 65–88 s, which reached a plateau after approximately 180 s (Fig. 1a). By 4 min, MPAP had increased significantly by 31 ± 5%, in spite of a small, albeit not significant, decline in both HR (6 ± 1%) and CO (16 ± 6%), reflecting substantial pulmonary vasoconstriction (67 ± 13% increase in PVR). Acute hypoxia also provoked a 56 ± 2% decrease in MABP by the end of the 4th min, which was primarily due to systemic vasodilatation (46 ± 3% decrease in SVR; Fig. 1a). Although CH slightly altered baseline values (detailed above), the magnitude of the response to 4 min hypoxia for MABP, HR, CO and SVR was essentially the same for the CH and N groups of rats (Fig. 1a,b). However, the potent pulmonary vasoconstriction seen in N rats was abolished in CH rats. Consequently, exposure to 10% O_2 did not cause a significant increase in MPAP or PVR in CH rats.

Administration of L-NAME

The maximum cardiovascular responses following a single i.c.v injection of L-NAME are given in Table 2. In N rats, L-NAME caused a small (<3% increase) but consistent increase in PVR ($P < 0.05$), although MPAP was not significantly affected. In addition, L-NAME caused a maximal 15 ± 4% increase in MABP after 35 ± 8 s, which was solely attributed to systemic vasoconstriction (16 ± 4% increase in SVR). All other variables were unaltered. The PVR, MABP and SVR responses were brief, returning to pre-L-NAME values within 4.5 min. Consequently, because acute hypoxia was tested 5 min after L-NAME injection, the prehypoxia baseline data were similar before and after L-NAME treatment. Furthermore, the magnitude of the cardiovascular responses to L-NAME for CH rats was statistically similar to that of N rats (Table 2). The i.c.v. administration of L-NAME did

Table 1 Baseline cardiovascular variables in rats exposed to normoxic or chronic hypoxia

	N rats	CH rats
MPAP (mmHg)	20.2 ± 1.1	30.4 ± 1.2**
MABP (mmHg)	106 ± 6	118 ± 4
CO (mL/min/100 g)	11.17 ± 0.75	12.32 ± 0.53
HR (b.p.m.)	416 ± 8	379 ± 11*
SVR (mmHg/mL per min per 100 g)	9.73 ± 0.64	9.72 ± 0.53
PVR (mmHg/mL per min per 100 g)	1.88 ± 0.14	2.52 ± 0.15*
RV/LV + Septum	0.31 ± 0.01	0.55 ± 0.02**
Haematocrit (%)	47 ± 1	65 ± 1**

Data are the mean±SEM. *$P < 0.01$, **$P < 0.001$ compared with normoxia values.

N, normoxic rats (groups 1 and 3; $n = 12$); CH, chronic-hypoxic rats (12% O_2 for 2 weeks; groups 2 and 4; $n = 11$); MPAP, mean pulmonary arterial pressure; MABP, mean arterial blood pressure; CO, cardiac output; HR, heart rate; SVR, systemic vascular resistance; PVR, pulmonary vascular resistance; RV, right ventricle; LV, left ventricle.

Table 2 Maximum responses to intracerebroventricular N^G-nitro-L-arginine methyl ester (150 μg in 10 μL) in normoxic rats ($n = 7$) and chronic hypoxic rats ($n = 5$)

	Normoxia		Chronic hypoxia	
	Pre-L-NAME	Max L-NAME	Pre-L-NAME	Max L-NAME
MPAP (mmHg)	18.6 ± 0.6	19.0 ± 0.6	30.4 ± 1.6	31.1 ± 1.9
MABP (mmHg)	102 ± 10	116 ± 8**	110 ± 5	120 ± 5*
CO (mL/min per 100 g)	10.12 ± 1.10	10.09 ± 1.13	12.24 ± 1.07	11.98 ± 1.00
HR (b.p.m.)	413 ± 10	416 ± 9	373 ± 13	376 ± 14
SVR (mmHg/mL per min per 100 g)	10.79 ± 1.85	12.39 ± 2.05**	9.14 ± 0.55	10.19 ± 0.66*
PVR (mmHg/mL per min per 100 g)	1.94 ± 0.20	2.00 ± 0.21*	2.53 ± 0.18	2.64 ± 0.21*

Data are the mean±SEM. *$P < 0.05$, **$P < 0.01$ compared with pre-N^G-nitro-L-arginine methyl ester (L-NAME).

MPAP, mean pulmonary arterial pressure; MABP, mean arterial blood pressure; CO, cardiac output; HR, heart rate; SVR, systemic vascular resistance; PVR, pulmonary vascular resistance.

not alter the acute hypoxic response for any of the variables recorded in either N or CH rats (Fig. 1a,b).

Cardiovascular responses to the i.v. administration of L-NAME (50 mg/kg, i.v.) were also recorded. In N rats, a bolus i.v. dose of L-NAME provoked robust systemic vasoconstriction (123 ± 20% increase in SVR; $P < 0.001$), as well as, to a lesser extent, pulmonary vasoconstriction (80 ± 10% increase in PVR; $P < 0.01$). The baroreflex decrease in HR and CO (NS; see baseline data in Fig. 1a,b) meant that the changes in vascular resistance were accompanied by smaller, but still significant, increases in MABP (42 ± 18% increase in MABP; $P < 0.001$) and MPAP (13 ± 9% increase in MPAP; NS) in N rats. After 2 weeks of chronic hypoxia, L-NAME (i.v.) had a similar effect on the systemic vasculature and caused a similar depression of HR (NS) and CO ($P < 0.001$), but it had a more pronounced effect on the pulmonary vasculature (24 ± 5% increase in MPAP (NS); 116 ± 18% increase in PVR ($P < 0.01$)).

Treatment of N rats with L-NAME (i.v.) exacerbated the reduction in MABP and SVR in response to acute hypoxia and accentuated the increase in MPAP and PVR (Fig. 1a,b). Despite a depression in baseline values for CO and HR, i.v. administration of L-NAME did not change the transient responses to hypoxia. In CH rats, the transient MABP and SVR responses to acute hypoxia were elevated by L-NAME (i.v.). In addition, L-NAME restored the potent MPAP (and PVR) response to acute hypoxia (observed in N rats), which had been absent prior to L-NAME treatment (Fig. 1a,b).

Administration of SIN-1

Following a single bolus i.c.v. injection of SIN-1 (100 μg) in N rats, baseline MPAP and PVR were not significantly altered. However, MABP declined slowly before stabilizing 38 ± 7% below the pre-SIN-1 baseline (Table 3). Preliminary studies

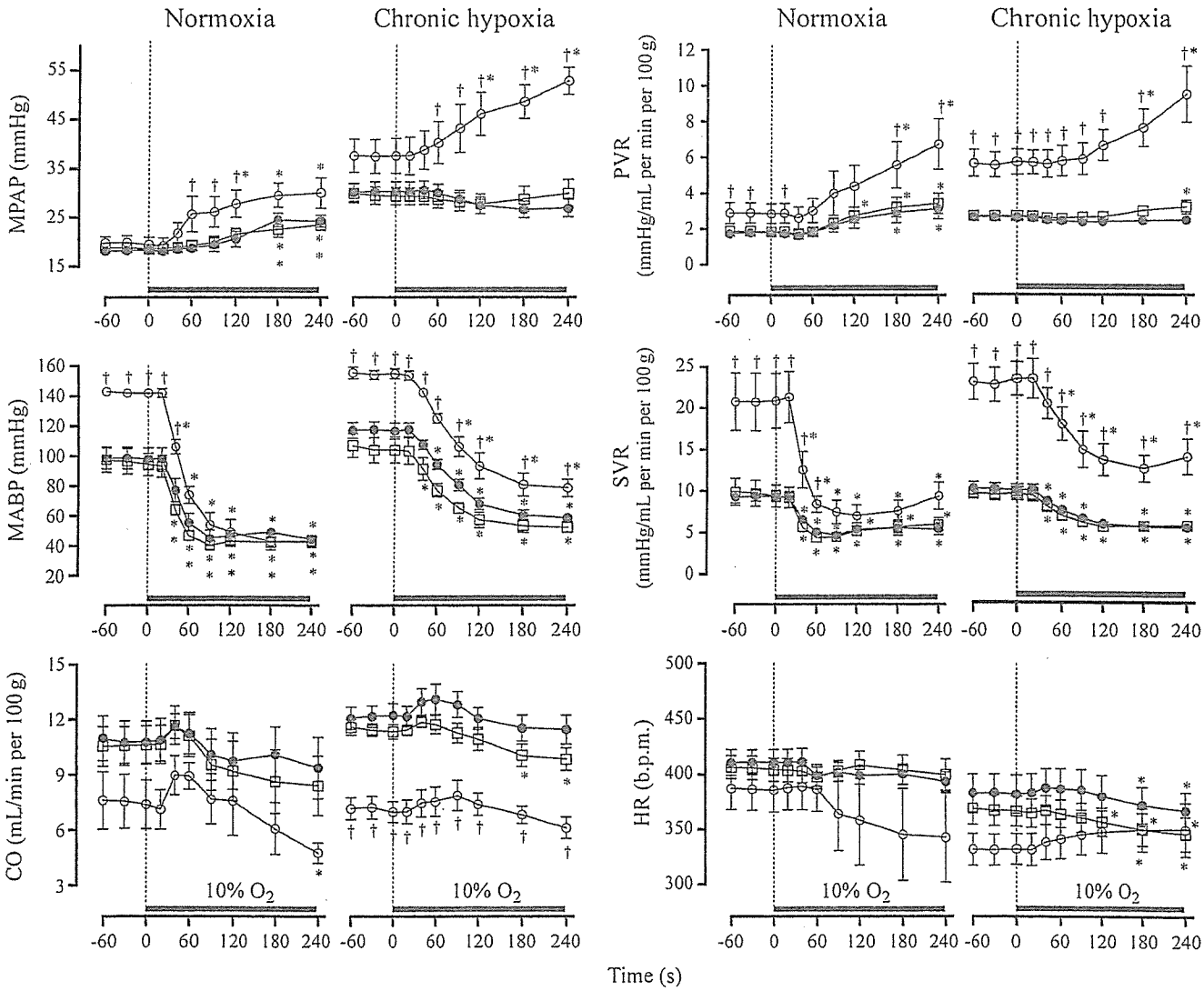

Fig. 1 Mean pulmonary arterial pressure (MPAP), mean arterial blood pressure (MABP), cardiac output (CO), pulmonary vascular resistance (PVR), systemic vascular resistance (SVR) and heart rate (HR) responses to acute hypoxia (10% O_2 for 4 min) in normoxic (N) rats ($n = 7$) and chronic hypoxic (CH) rats ($n = 5$), before (●) and after the administration of N^G-nitro-L-arginine methyl ester (L-NAME; □, 150 μg in 10 μL, i.c.v.; ◇, 50 mg/kg, i.v.). $^*P < 0.05$ compared with pre-acute hypoxia values; $^\dagger P < 0.05$ compared with L-NAME values.